I. J. Engineering and Manufacturing, **2025, 2, 1-18**
Published Online on April 8, 2025 by MECS Press (http://www.mecs-press.org/)
DOI: 10.5815/ijem.2025.02.01

Liquefaction Susceptibility of Earthworks Site: Numerical Modelling of Embankment Cut by PLAXIS2D and GEOSLOPE Using Eurocode 7

Sheeraz Ahmed Rahu*
Department of Geotechnics and Engineering Geology, Budapesti Műszaki és Gazdaságtudományi Egyetem, Műegyetem rakpart 3., Budapest 1111 Hungary
E-mail: sheerazahmed.rahu@edu.bme.hu
ORCID iD: https://orcid.org/0000-0002-7026-1471
*Corresponding Author

Zaheer Ahmed Almani
Department of Civil Engineering, Mehran University of Engineering and Technology, Pakistan
E-mail: zaheer.almani@faculty.muet.edu.pk
ORCID iD: https://orcid.org/ 0000-0002-1579-5681

Muhammad Rehan Hakro
Department of Civil Engineering, Mehran University of Engineering and Technology, Pakistan
E-mail: rehan.hakro@faculty.muet.edu.pk
ORCID iD: https://orcid.org/0000-0003-4740-6588

Received: 10 May, 2024; Revised: 15 June, 2024; Accepted: 11 August, 2024; Published: 08 April, 2025

Abstract: This paper presents a comprehensive study encompassing both liquefaction susceptibility evaluation and slope stability analysis of embankment soil adjacent to road. The paper focuses on the vulnerability of embankment soil to liquefaction-related failures. It examines the liquefaction vulnerability of embankments ML-CL soil, previously considered non-liquefiable but raising concerns post-1999 Kocaeli Earthquake. The paper evaluates liquefaction susceptibility using Chinese Criteria and Modified Chinese Criteria based on index test results of embankments soil samples. The soil at various depths was found to be not susceptible to liquefaction as per Chinese criteria, whereas the second evaluation as per Modified Chinese criteria gave different and more specific results taking into the % clay-sized particles. Based on Modified Chinese criteria, the soils ranging from 10-20 ft, 25-30 ft and 30-35 ft were found explicitly non-susceptible, whereas soil ranging from 0-10 ft and 20-25 ft requires further study on non-plastic clay-sized grains as per the criteria. The paper delves into slope stability analysis using PLAXIS2D and GEOSLOPE software to determine the optimal earthworks layout for a embankment excavation based on Eurocode 7. Upon numerical modelling, various trials were carried out considering various factors of safety across different earthworks layouts and the one with satisfying factor of safety is considered safest, ensuring safety and cost-effectiveness of embankment cut besides the road.

Index Terms: Liquefaction Susceptibility, Slope Stability, ML-CL, PLAXIS2D, GEOSLOPE, Optimal Layout, Eurocode 7

1. Introduction

This paper offers an in-depth study that evaluates the susceptibility of embankment soil to liquefaction and assesses the stability of slopes adjacent to a road. The study specifically focuses on the ML-CL embankment soil, which was previously deemed non-liquefiable but became a concern after the 1999 Kocaeli Earthquake. Liquefaction susceptibility was assessed using the Chinese Criteria and the Modified Chinese Criteria, based on index test results from soil samples. According to the Chinese Criteria, the soil at various depths was found to be non-liquefiable. However, the Modified Chinese Criteria, which consider the percentage of clay-sized particles, provided different and more detailed results. Soils at depths of 10-20 ft, 25-30 ft, and 30-35 ft were found to be explicitly non-liquefiable, whereas soils at depths of 0-10 ft and 20-25 ft require further examination of non-plastic clay-sized particles [1].

Additionally, the paper explores slope stability using PLAXIS2D and GEOSLOPE software to find the best earthworks layout for an embankment excavation, following Eurocode 7 standards. Through numerical modelling and multiple trials, the study identified the layout with an adequate safety factor, ensuring both safety and cost-efficiency for the embankment cut beside the road [2].

In a broader perspective, modern engineering must address the safety of structures, which are often threatened by unpredictable disasters. Many failures result from the instability of soil masses, with liquefaction being a major cause. Historical incidents, such as the 1964 earthquakes in Alaska and Niigata, demonstrated the severe impact of liquefaction, including slope failures and the destruction of infrastructure. Liquefaction causes soil to act like a liquid, compromising stability during events like earthquakes, blasting, or pile driving. This highlights the importance of identifying vulnerable soils. Building on previous geotechnical research, particularly studies following the 1999 Kocaeli Earthquake, this paper analyzes suspected liquefiable embankment soil using both the Chinese and Modified Chinese Criteria. The method involved percussion boring to a depth of 35 ft, with the groundwater table at 5 ft from the ground surface at the slope's toe [1].

Modern Liquefaction research is backed up by earthquakes like 1964 Nigata and Alaska Earthquakes. Every new earthquake opens a door for new research area.

The Liquefaction susceptibility of any soil layer depends upon following factors;[3]

1. Soil Type
2. Relative Density
3. Particle Size distribution
4. Hydraulic conductivity or Permeability of Soil
5. % Plastic fines
6. Age and Cementation
7. Overburden pressure or Historical liquefaction
8. Environment of deposition
9. Location of Ground Water Table
10. Earthquake Intensity and duration

Liquefaction Susceptibility Criterions:

Particularly for ML-CL type fine grained soils, following are some of the major liquefaction susceptibility criterions,

1. Chinese Criteria and Modified Chinese Criteria (shown in Figure 1 and 2 respectively)
2. Andrews and Martin (2000)
3. Youd et al. (2001)
4. Seed et al. (2003)
5. Bray et al. (2004)
6. Bray and Sancio (2006)
7. Boulanger and Idriss (2006) etc

This research would be employing Chinese criteria and Modified Chinese criteria.

1.1. Chinese Criteria

Introduction: Wang (1979) studied the liquefied soils after 1975 Haicheng Earthquake and 1976 Tangshan in China and compared the soils of both Earthquakes and found out the Soil characteristics, and afterwards was devised by Seed et. al. into three limits or criterions [4].

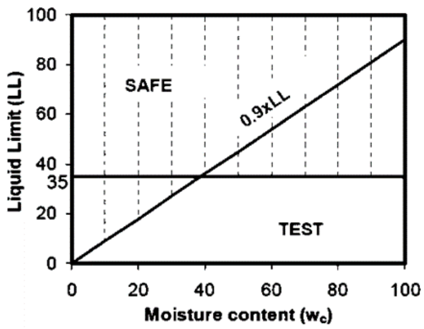

Fig. 1. Chinese Criteria after Wang [5]

1.2. Modified Chinese Criteria

Introduction: This was modification of Chinese criteria, in which (Koester 1992) recommended using Casagranda for determination of liquid limit after its reduction, and then (Andrews and Martin 1999) used 0.2 micrometre as limit between clay and silt particles, and set Liquid limit criteria based on Casagranda apparatus [4].

Clay Content	**Liquid Limit < 32%**	**Liquid Limit ≥ 32%**
< 10%	Susceptible	Further studies required (considering plastic non clay sized grain - mica)
>10%	Further studies required (considering non plastic clay sized grain – mine and quarry tailings)	Not susceptible

Fig. 2. Modified Chinese Criteria [6]

In first phase, determinations of engineering properties of embankment soil were carried out in order to investigate the strength of embankment soil and its strength parameters, consequently categorization of embankment soil was done accordingly, whereas in phase two, the embankment soil underwent the classification based on particle size distribution by use of hydrometer analysis. Moreover, Atterberg's limits (consistency limits) of embankment soil were also determined. These preliminary tests help classify and later evaluate the liquefaction susceptibility of soil of formation [7]

1.3. Methodology Flowchart

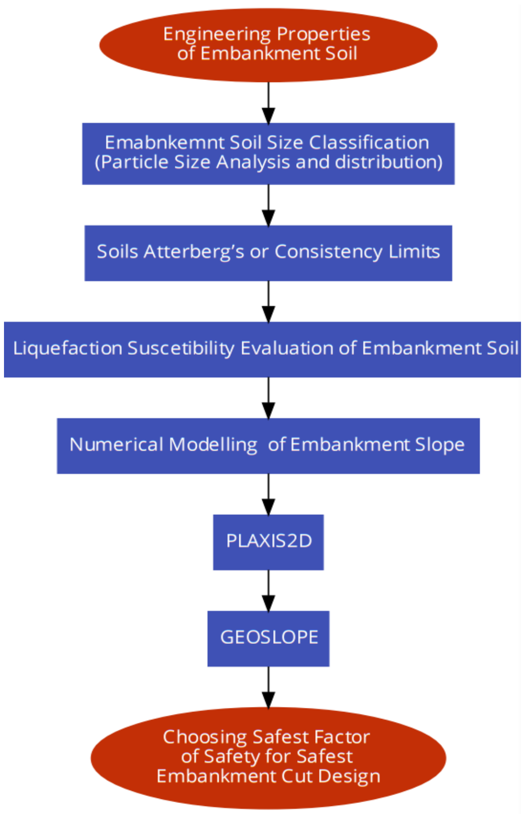

1.4. Engineering Properties

Firstly, it includes the assessment of engineering behaviour of embankment soil, such as stress-strain characteristics and shear strength of embankment soil by using;

1. Unconfined Compression Test (Uni-axial Compression Test) (as shown in Figure 3)
2. Direct Shear Test (as shown in Figure 4)

Fig. 3. Application of Load in UTM Machine, Geotechnical Engineering Laboratory, 2020

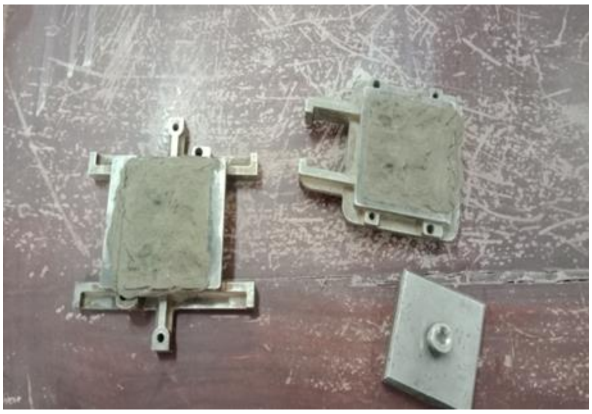

Fig. 4. Direct Shear Test Sheared Specimens, Geotechnical Engineering Laboratory, 2020

Secondly, it includes the tests for classification of embankment soil, based on AASHTO system of classification, which require;

1. Particle Size Analysis and distribution (using Hydrometer analysis)
2. Consistency or Atterberg's limits (only Plastic limit & Liquid limit)

As the embankment soil under observation was fine-grained soil (ML-CL), since No. 200 passing was found out to be greater than 50%, hence the hydrometer analysis was employed to check particle size distribution. Further as the criterions used under this research head required only Liquid limit and plastic limit, hence the work was limited in that context.

1.5. Unconfined Compression Test

Representative Depth of Sample: 0 to 10 ft"
Trial #1
Readings for Unconfined Compression test (Trial 1)
(Height = H = 10.2cm & Diameter = D =5.1cm)
Proving Ring Constant = 0.125

Table 1. Dial Guage Readings for Unconfined Compression test

Time (seconds)	Dial Gauge Reading	Deformation (mm)	Dial Gauge Reading
15	55	0.55	1
75	238	2.38	7
150	471	4.71	13.5
225	700	7	20
300	905	9.05	23
375	1125	11.25	28
450	1350	13.5	32
525	1565	15.65	35.5
600	1775	17.75	38.2
675	1990	19.9	40.9
750	2210	22.1	43.5

In the unconfined compression test (as shown in readings in Table 1), we assume that no pore water is lost from the embankment soil sample during set-up or during the shearing process. A saturated sample will thus remain saturated during the test with no change in the sample volume, water content, or void ratio. More significantly, the sample is held together by an effective confining stress that results from negative pore water pressures (generated by menisci forming between particles on the sample surface).

Table 2. Compressive Strength upon gradual loading

Load (kg)	Strain	Corrected Area (cm^2)	Compressive Strength (kg/cm^2)
0.125	0.005	20.54	0.006
0.875	0.023	20.92	0.042
1.6875	0.046	21.42	0.079
2.5	0.069	21.93	0.114
2.875	0.089	22.42	0.128
3.5	0.11	22.96	0.152
4	0.132	23.54	0.17
4.4375	0.153	24.13	0.184
4.775	0.174	24.73	0.193
5.1125	0.195	25.38	0.201
5.4375	0.217	26.08	0.209

Pore pressures are not measured in an unconfined compression test; consequently, the effective stress is unknown. Hence, the undrained shear strength measured in an unconfined test is expressed in terms of the total stress as shown in readings in Table 2. These values were plotted into stress-strain graph as shown in Figure 5.

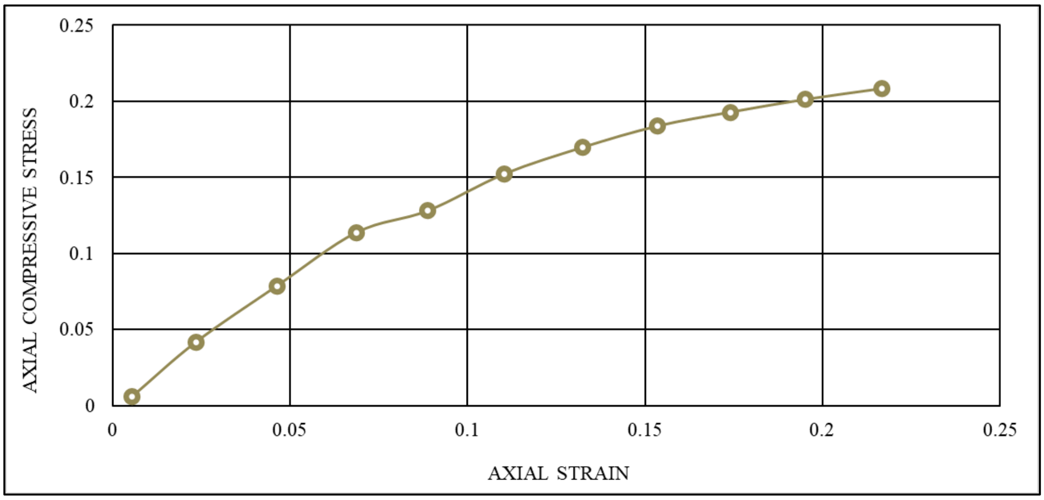

Fig. 5. Axial Strain VS Axial Compressive Stress

Subsequently three more trials were attempted for embankment soil samples from 10 to 35 ft. Following values of maximum compressive Strength and undrained Shear Strength were obtained from each trial as shown in Table 3.

Table 3. Shear Strength

Trial No.	Compressive Strength, q (kPa)	Shear Strength, S_u (kPa)
1	20.4958985	10.24794925
2	20.7312581	10.36562905
3	21.378497	10.6892485
4	32.89248477	16.44624238
Average Compressive Strength (kPa)		Average Shear Strength (kPa)
23.87453459		11.9372673

The value obtained above for average compressive strength in kPa as tabulated above in Table 3 can be employed in establishing relationship between the strength of embankment soil in terms of consistency. Table 4 below gives relationship between the average compressive strength of soil.

Table 4. Relationship between consistency and unconfined compression strength

Consistency	q_u (kPa)
Very Soft	0-25
Soft	25-50
Medium Stiff (firm)	50-100
Stiff	100-200
Very Stiff	200-400
Hard	>400

Since the value of average compressive strength of embankment soil of representative depth of 0-10 ft lies in range of 0-25 kPa, Hence the description of consistency of embankment soil would be “Very Soft”.

1.6. Direct Shear Test

“Representative Depth of Sample: 0 to 10 ft”

Sample 1 (Normal Load/Vertical Load = 24.5 kg) (Rate of Strain or Horizontal Displacement = 0.05mm/min) (Proving Ring Constant for Horizontal Dial Gauge Readings = 0.15) (Vertical Dial Gauge Readings are 1/100th of mm)

Table 5. Dial Guage Readings for Direct Shear test

Time (seconds)	Horizontal Dial Gauge Readings (HDG)	Vertical Dial Gauge Readings (VDG)
15	2	0
300	31.9	0.001
600	59.5	4.1
900	73.5	6.9
1200	85	8.5
1500	96	9.3
1800	107	9.9
2100	117.1	9.95
2400	125.3	9.95
2700	132.5	9
3000	139.6	7.6
3300	144.2	6.5
3600	157.9	4.8
3900	151.5	2.9
4200	153.8	1.2

Employing Strain-controlled Direct Shear equipment, which helped in yielding both Peak and residual strengths as shown in Table 6. Most suitable for consolidated drained test.

Table 6. Strain controlled Direct Shear Stresses

Shear Force (kg) =HDGx0.15	**Shear Stress (kg/cm²)**
0.3	0.008333333
4.785	0.132916667
8.925	0.247916667
11.025	0.30625
12.75	0.354166667
14.4	0.4
16.05	0.445833333
17.565	0.487916667
18.795	0.522083333
19.875	0.552083333
20.94	0.581666667
21.63	0.600833333
23.685	0.657916667
22.725	0.63125
23.07	0.640833333

Also using the vertical and horizontal dial gauge readings in Table 5, deformations were calculated as shown in Table 7.

Table 7. Vertical Deformation

Vertical Deformation (mm) = VDG x0.01	**Horizontal Displacement (cm) = HDG x 0.05mm/min**
0	0.0125
0.00001	0.025
0.041	0.05
0.069	0.075
0.085	0.1
0.093	0.125
0.099	0.15
0.0995	0.175
0.0995	0.2
0.09	0.225
0.076	0.25
0.065	0.275
0.048	0.3
0.029	0.325
0.012	0.35

To facilitate the re-molding purpose, an embankment soil sample may be compacted at optimum moisture content in a compaction mold. Then specimen for the direct shear test could be obtained using the correct cutter provided.

The values obtained were plotted in shear stress-shear displacement graph as shown in Figure 6.

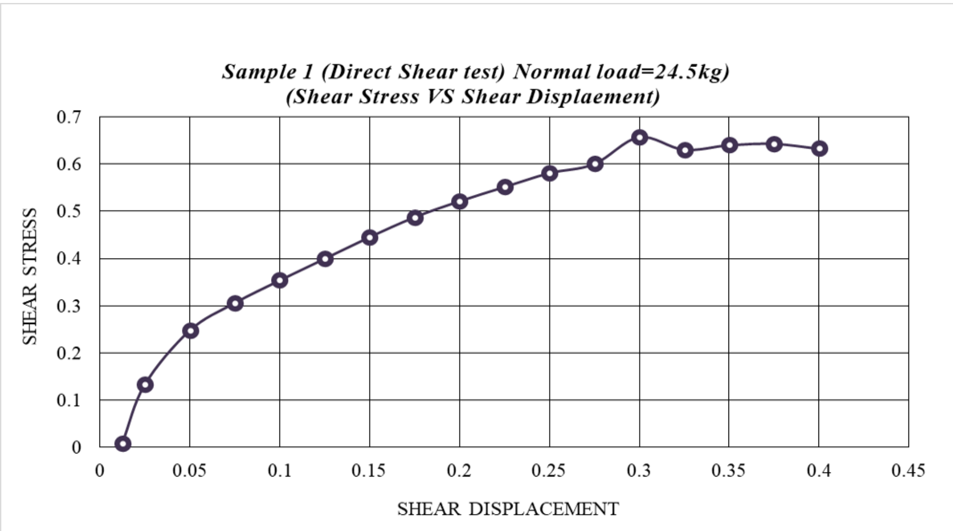

Fig. 6. Stress VS Displacement Graph

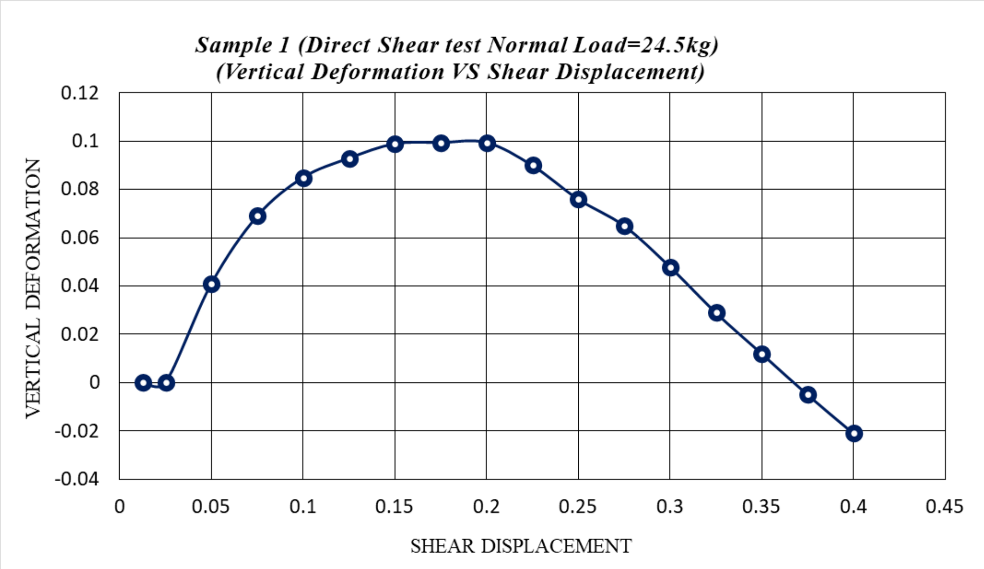

Fig. 7. Vertical Deformation VS Shear Displacement Graph

Similarly, the dial gauge readings were plotted in vertical deformation vs shear displacement graph as shown in Figure 7. Measurements of shear load, shear displacement and normal displacement are recorded. The test is repeated for two or more identical specimens under different normal loads (44.5 kg and 84.5 kg). From the results, shear strength parameters can be determined. The values below in Table 8 can be used to plot the Failure envelop.

Table 8. Direct Shear test Results

Normal Stress (kg/cm^2)	Shear Stress (kg/cm^2)
0.68056	0.657916667
1.236	1.133333333
2.3472	1.995833333

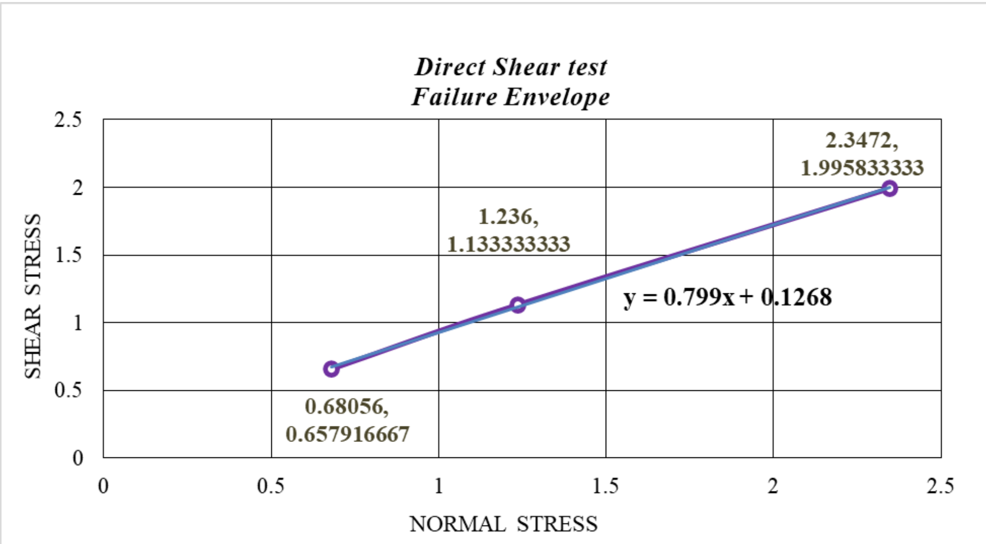

Fig. 8. Direct Shear Test plot

From the failure envelop in Figure 8, it can be observed "$\tau = 0.799\sigma + 0.1268$"
Since $\tau = (tan\emptyset)\sigma + c$
So $tan\emptyset = 0.799 \rightarrow \emptyset = tan^{-1}(0.799) \rightarrow \emptyset = 38.6\,°$

$$Angle\ of\ Internal\ Friction = \emptyset = 38.6\,°$$
$$\&\quad Cohesion = c = 0.1268 kg/cm^2$$

Hence the embankment soil can be categorized as "$\boldsymbol{C - \emptyset}$" soil as per results obtained from Direct Shear test.

2. Soil Classification

1. Particle Size Analysis and distribution (using Mechanical Sieving and Hydrometer analysis)

As the embankment soil under observation was fine-grained soil (ML-CL), since No. 200 passing was found out to be greater than 50%, hence the hydrometer analysis was employed to check particle size distribution.

Since, to establish a decision to whether the given embankment soil is susceptible to liquefaction or not, the % fines (<0.005mm) and % clay-sized particles were required as per Chinese and Modified Chinese criteria. Hence the particle size distribution was performed first by use of mechanical sieving and then by hydrometer analysis, to establish the particle size distribution curves as shown in Figure 9 for various representative depths and to determine the % particles of various sizes as per USCS and AASHTO standards in the section ahead.[8]

Hydrometer analysis covers the quantitative determination of the particle size distribution in embankment soil from a coarse sand size to the clay size by the means of sedimentation. The test is normally not required if less than 10% of the material passes the 75µm test sieve. The hydrometer analysis is based on Stokes' Law.[9]

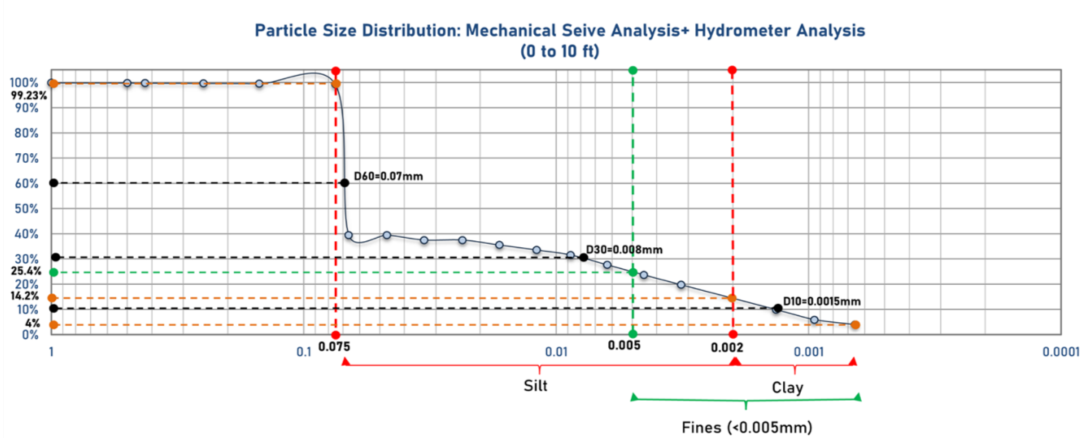

Fig. 9. Particle Size Distribution

Table 9. Passing Grain Size and Coefficients

Depth of Sample	D60 (mm)	D30 (mm)	D10 (mm)	Cu Coefficient of Uniformity	Cc Coefficient of Curvature
0-10 ft	0.07	0.008	0.0015	47	0.61
10-20 ft	0.065	0.0065	0.001	65	0.65
20-25 ft	0.067	0.004	0.0017	39	0.14
25-30 ft	0.067	0.0045	0.0015	45	0.20
30-35 ft	0.02	0.0035	0.0015	13	0.41

Table 10. AASHTO Particle Size Classification

Depth of Sample	Highest % passing (0.075mm)	% passing (0.005mm)	% passing (0.002mm)	Lowest % passing (<0.002mm)	Silt Content = Col:2-Col:4	Clay Content = Col:4-Col:5	%Fines (<0.005mm) = Col:3-Col:5	AASHTO Particle Size Classification remark
0-10 ft	99.23%	25.4%	14.2%	4%	85.02%	10.2%	21.4%	Clay and Silt
10-20 ft	99.23%	27%	17.5%	4%	81.7%	13.5%	23%	Clay and Silt
20-25 ft	99.23%	32%	12%	3.94%	87.23%	8.06%	28.06%	Clay and Silt
25-30 ft	99.23%	32%	17.5%	5.9%	81.73%	11.6%	26.1%	Clay and Silt
30-35 ft	99.23%	42%	15.8%	4%	83.43%	11.8%	38%	Clay and Silt

As observed in above values tabulated in Table 9 and 10 which were obtained from assembled results of Mechanical Sieve Analysis and Hydrometer Analysis, following remarks were made as per AASHTO;

a. As per AASHTO, the embankment soil belongs to silt-clay material category type soils, as No.200 passing observed was greater than 35% as can be seen in Table.

b. Further, the particle size distribution curves helped in determining relative Silt and Clay contents to help name the embankment soil as Clayey Silt based on percentage composition.
c. Further, the particle size distribution curves indicated that embankment soil varies from well-graded at shallow depths to uniformly graded at greater depths.

Atterberg's or Consistency Limits

Liquid Limit

Embankment soil specimen for the liquid limit test was collected from the representative samples by passing the soil from the #40 sieve. The specimen was then checked for their liquid limits using Casagranda Type Liquid Limit Apparatus (ASTM D4318). Three trials were made for each sample (at 10-20, 20-30, 35-45 blows respectively) so as to obtain the blows vs. water content (w) plot as shown in Figure 10. Thereafter, the water content (wc) corresponding to the 25 blows was determined from the graph plot of the recorded test data. [10]

Plastic Limit

Embankment soil specimens for the Plastic Limit (PL) test were collected from the representative samples by passing the soil from the #40 sieve. The soil specimen were then checked for their plastic limit by the rolling threads method, wherein the samples were checked by rolling the soil-water mix on the glass plate and rolled until the threads crumbled or cracks appeared on them. The crumbled soil thread samples were then oven dried to check for their water content (w). The process was repeated three to four times for each sample and the average corresponding water content was determined. Thus, the average water content found was the plastic limit of the particular soil sample as shown in Table 11.

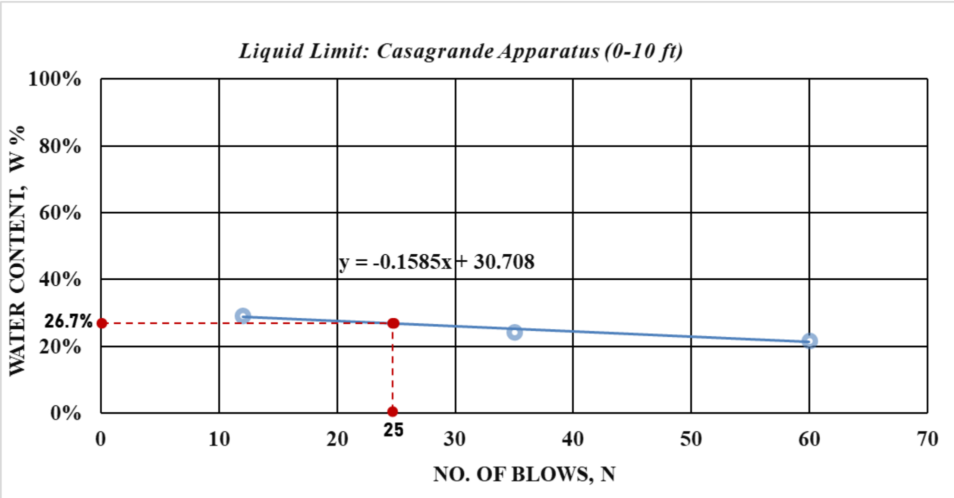

Fig. 10. Liquid Limit by Casagrande Apparatus

Table 11. Plasticity Indices

Representative Depth	Liquid limit	Plastic limit	Plasticity index
0-10 ft	26.7%	14.935%	11.765
10-20 ft	34.8%	15.17%	19.63
20-25 ft	38.7%	24.4318%	14.2682
25-30 ft	36.8%	24.418%	12.38
30-35 ft	36.6%	25.3474%	11.25

Liquefaction Susceptibility of Soil

Liquefaction susceptibility of soils have been tabulated in Table 12-13 for Chinese and Modified Chinese criteria respectively.

Table 12. Chinese Criteria Results

Representative Depth	Fines (<0.005mm)	Liquid limit	Natural Water Content	Chinese Criteria Remarks
0-10 ft	21.4%	26.7%	21.43%	Not Susceptible to Liquefaction
10-20 ft	23%	34.8%	39.7%	Not Susceptible to Liquefaction
20-25 ft	28.06%	38.7%	33.33%	Not Susceptible to Liquefaction
25-30 ft	26.1%	36.8%	31.25%	Not Susceptible to Liquefaction
30-35 ft	38%	36.6%	25%	Not Susceptible to Liquefaction

Table 13. Modified Chinese Criteria Results

Representative Depth	Clay Content	Liquid limit	Modified Chinese Criteria Remarks
0-10 ft	10.2%	26.7%	Further studies required (considering non-plastic clay-sized grains -mine and quarry tailings)
10-20 ft	13.5%	34.8%	Not Susceptible to Liquefaction
20-25 ft	8.06%	38.7%	Further studies required (considering non-plastic clay-sized grains -mica)
25-30 ft	11.6%	36.8%	Not Susceptible to Liquefaction
30-35 ft	11.8%	36.6%	Not Susceptible to Liquefaction

3. Numerical Modelling of Embankment Cut by PLAXIS2D and GEOSLOPE in order to design an economical and safe angle of steep and foot length of embankment cut

Technical description of the model:

In order to design an economical and safe angle of steep and foot length of embankment cut as an earthworks for road project as shown in Figure 11. The Slope stability analysis uses PLAXIS2D and GEOSLOPE to determine optimal layout by determining various factors of safety for different layouts.

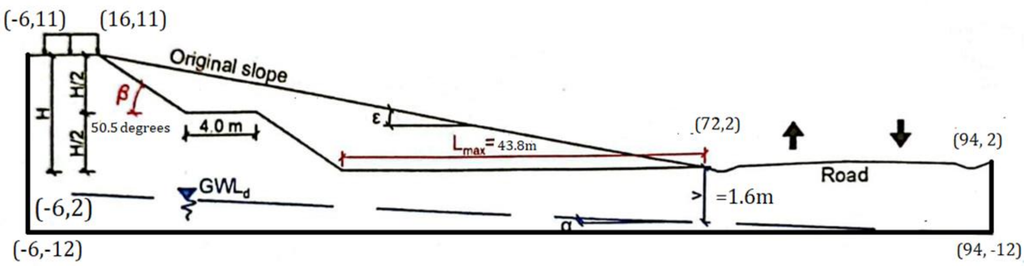

Fig. 11. Model Dimensions of the Embankment

3.1. PLAXIS2D:

For modelling, plain strain model with 15 noded elements was employed. The screen grid contour settings were initially set to the following dimensions considering the values *estimated with given slope angles.The scale of the grid has been set according to the dimensions of the project plus some screen clearance.*

$Xmax = Surcharge\ Width + Base\ of\ Slope + Road\ Width = 4m + \frac{H}{tan\varepsilon} + 12m =$ 4m $+ \frac{8}{tan10°} + 12m =$ $61.37\ \approx 62$

$Ymax = H + v + roadwidth(tan\alpha) = 8m + 1.6m + 12m\ (tan4°) = 10.44\ \approx 11m$

Based on the particle size distribution, the soil is assumed as silt, considering the major percentage passing. Further properties of soil have been tabulated in Table 14.

Table 14. Soil Model Properties

Soil Properties	
Soil type	Silt
Unit weight (γ)	$17.3\frac{kN}{m^3}$
Saturated Unit weight (γsat)	$19.2\frac{kN}{m^3}$
Angle of internal friction ($\emptyset$)	38.6°
Cohesion (C)	12 KPa
Oedometric Modulus E_{oed}	14.4 MPa
Poisson Ratio (Assume ϑ)	0.35
Elastic/Youngs Modulus $E = Eoed\ x\ \left(1 - \frac{2v^2}{1-v}\right)$	$3972\frac{KN}{m^2}$
Bulk Modulus $G = \frac{E}{2(1+v)}$	$3323\frac{KN}{m^2}$

3.1.1. Procedure adopted:

Plane Strain 15 noded model type is used along with metric units. The Soil type is silt with given values of bulk density, saturated density, oedometric modulus, cohesion and angle of internal friction and assumed value of poisson ratio is taken. Material properties were established based on following formulations.[11]

Assuming Poisson ratio of 0.35 for silt, we have

$$E = Eoed\ x \left(1 - \frac{2v^2}{1-v}\right)$$

$$G = \frac{E}{2(1+v)}$$

Following this, the slope was defined using Polygon option in structures tab and then cut was introduced using cut polygon option. Further polygon was modified using move polygon points option and move polygon line option. Upon constructing a polygon, material was assigned to both the embankments original slope and cut.

Afterwards, meshing was done using medium setting and results were viewed, however, very fine settings were also possible. Moreover, the Ground water table was introduced using Create water level option using points in Flow conditions tab. The gradient of GWT was set to 4 degrees with 1.6m distance to toe of the slope.

Furthermore, a construction of model was executed from initial stage to excavation with surcharge. This was done using staged construction tab in PLAXIS2D interface. Following settings were used in staged construction.

- Initial phase (calculation type is k0 procedure and the structure is activated in this
- phase)
- Stability prior to excavation (calculation type is plastic)
- Factor of safety for original slope (calculation type is safety)
- Excavation phase (calculation type is plastic, the cut is deactivated in this phase)
- Factor of safety without surcharge (calculation type is safety)
- Surcharge phase (calculation type is plastic and the surcharge load is activated)
- Factor of safety with surcharge (calculation type is safety)

Before starting calculation, a node was selected from the possible slip surface vantage point to observe the relationship between parameters like displacement and FOS through curves delineated above. Following this, the results for various parameters were viewed in Figure 12-16 and tabulated.

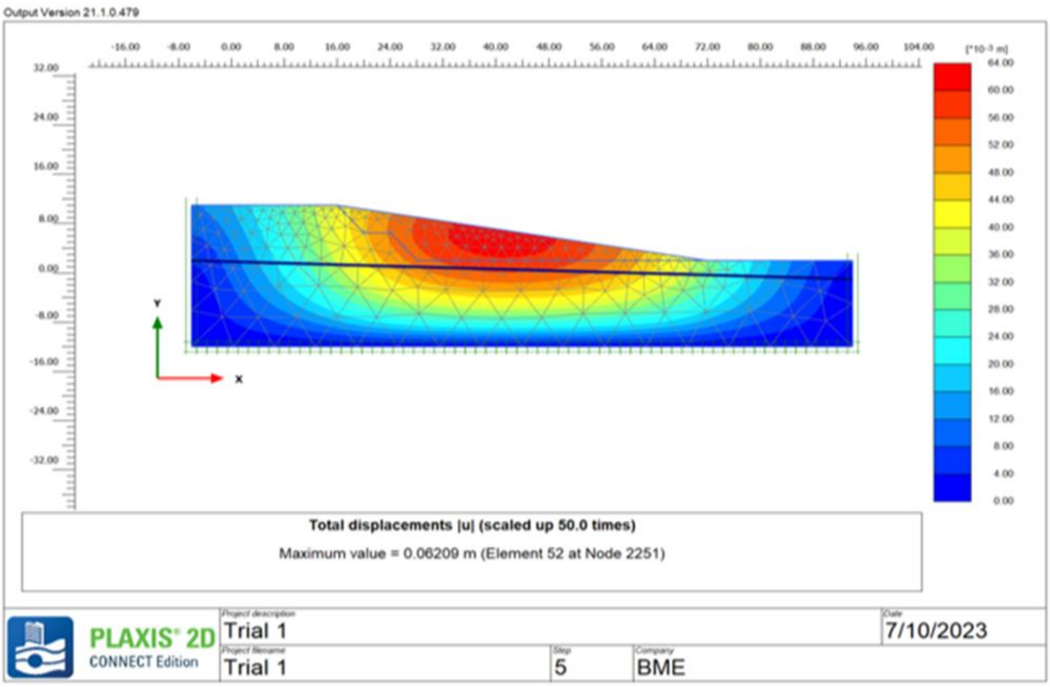

Fig. 12. Deformed Mesh under Surcharge

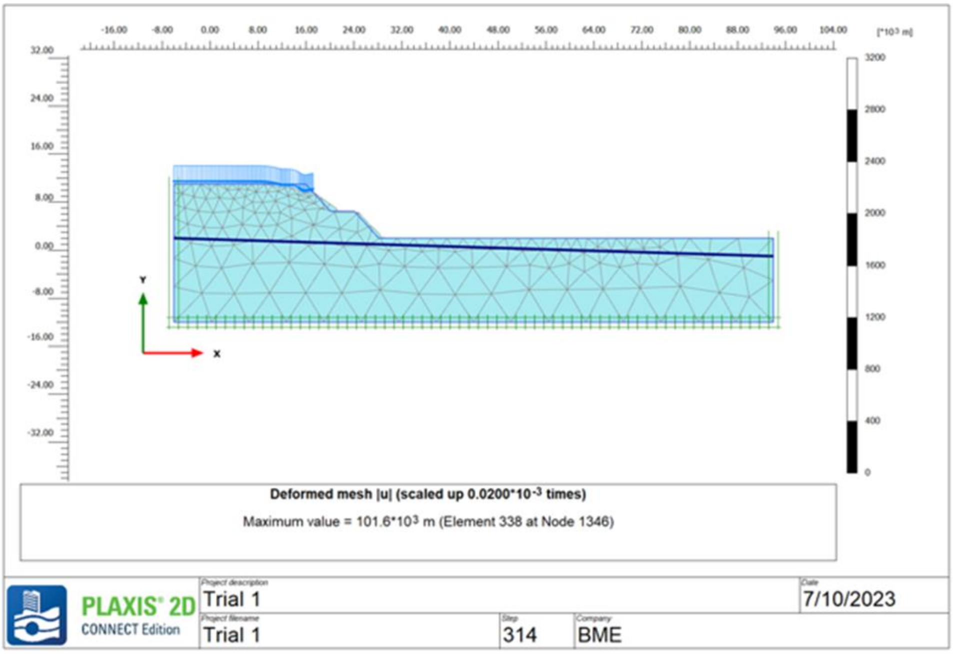

Fig. 13. Total Displacement Spectrum of Original Slope

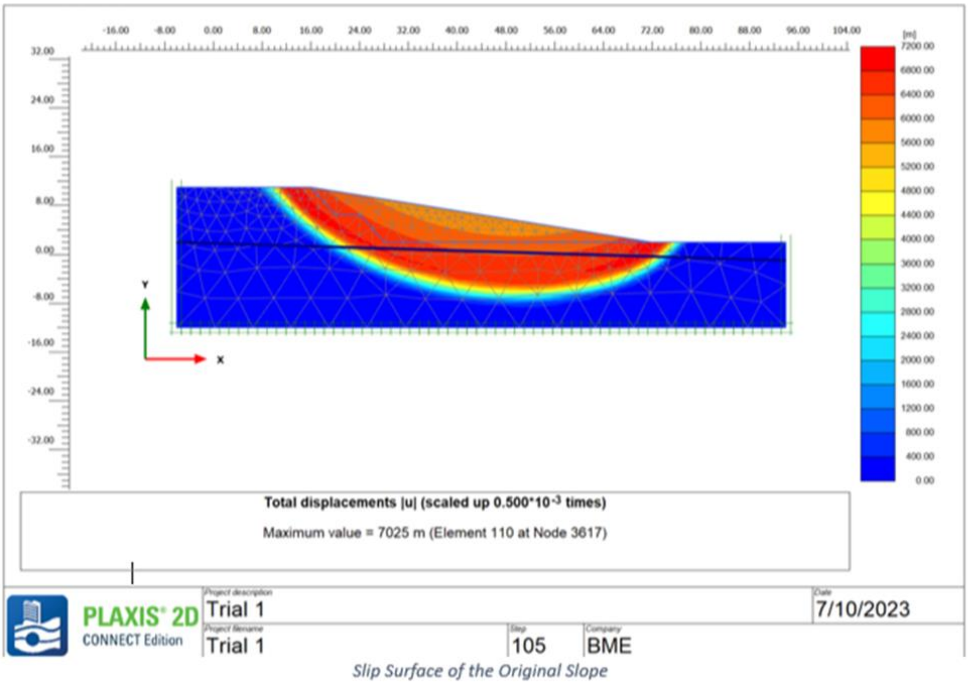

Fig. 14. Slip Surface of the Original Slope

Table 15. Optimal Model Design Selection

Model #	L_{max}	β	Original Slope	Without Surcharge	With Surcharge	Comments
1	43.8	50.5	3.374	1.424	1.354	Most Safe
2	32	21.8	3.389	2.135	2.035	Safe
3	23	19.6	3.390	2.481	2.387	Safe
4	18	16.4	3.390	2.742	2.636	Safe
5	16	14.6	3,394	2.816	2.717	Safe

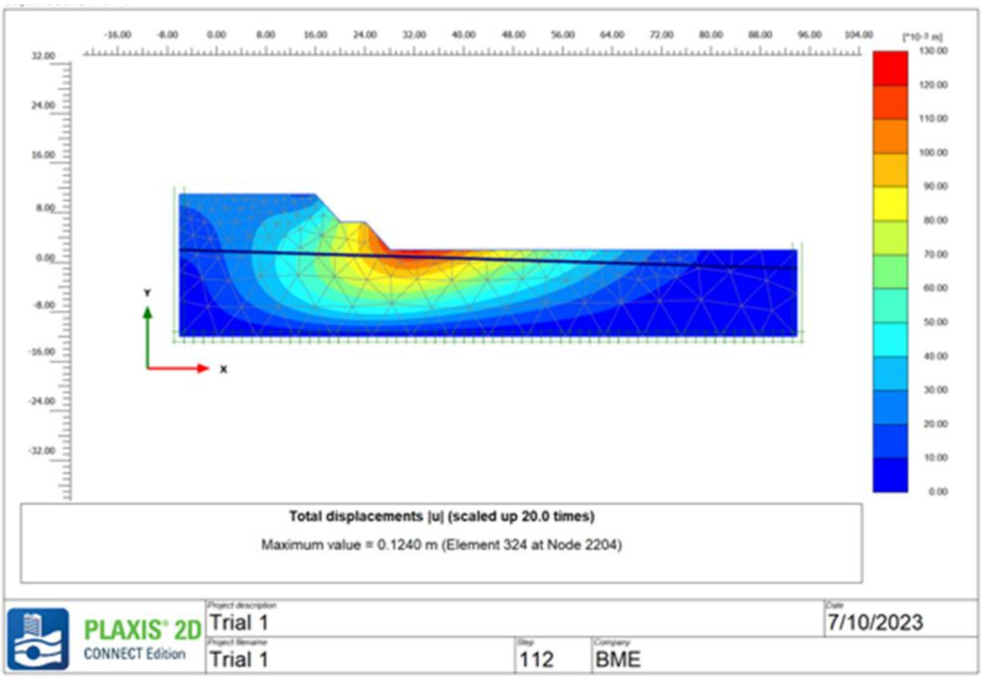

Fig. 15. Total Displacement Spectrum of Excavation

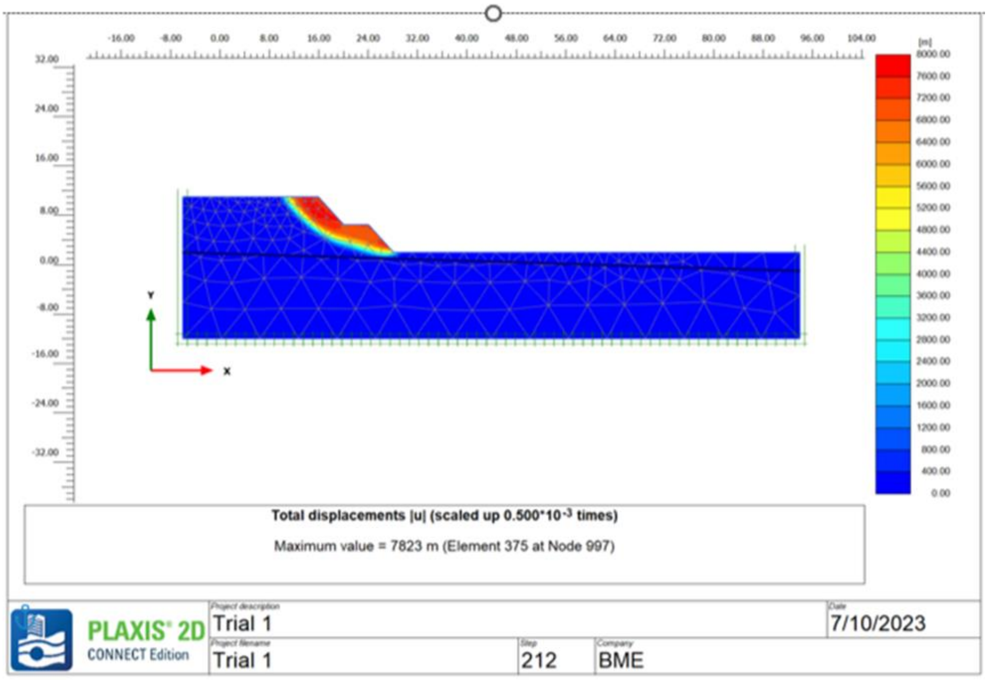

Fig. 16. Slip Surface of Excavation with Surcharge

Trial 1 in Table 15 is optimal since it also meets range of 1.35 to 1.38 for slope with surcharge.

The curves in Figure 17 represent the variation of a particular parameter (e.g., time, displacement, or any other relevant parameter) with respect to the construction stages. By defining a curve, you can control the timing and sequencing of construction activities. By using a curve in staged construction analysis, you can simulate the time-dependent behavior of construction stages, allowing for more realistic and controlled simulations of construction processes.

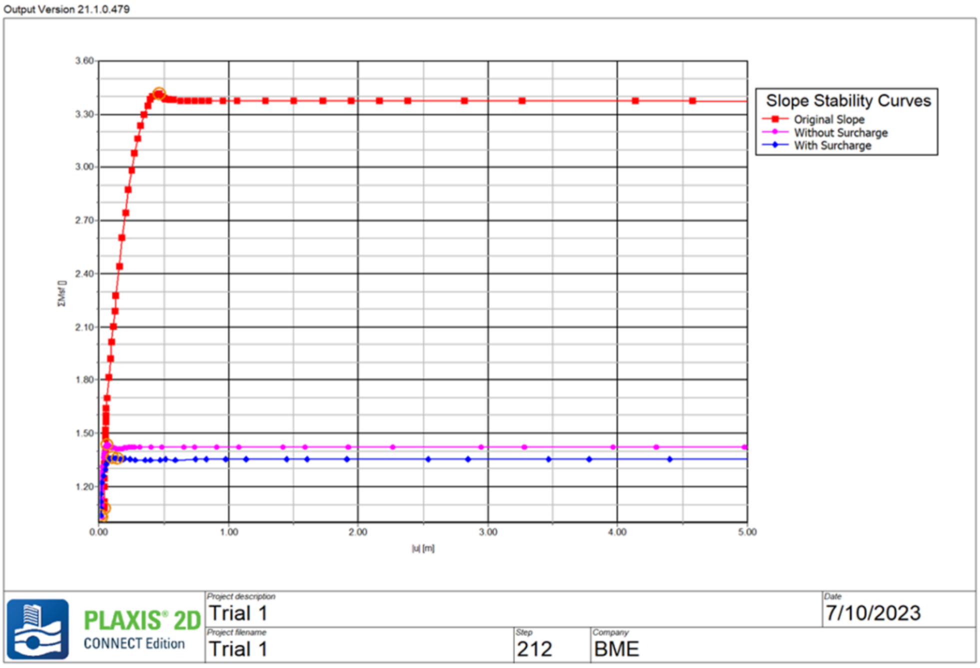

Fig. 17. Slope Stability Curves

Safety factors are not absolute values but are relative indicators of stability. They depend on the specific modeling assumptions and input parameters used in the analysis. Variations in the slope geometry, such as slope angle, slope height, and presence of irregularities, can affect the distribution of stresses and influence the factor of safety as observed in Figure 18-19. Different slope geometries can result in varying factor of safety values.

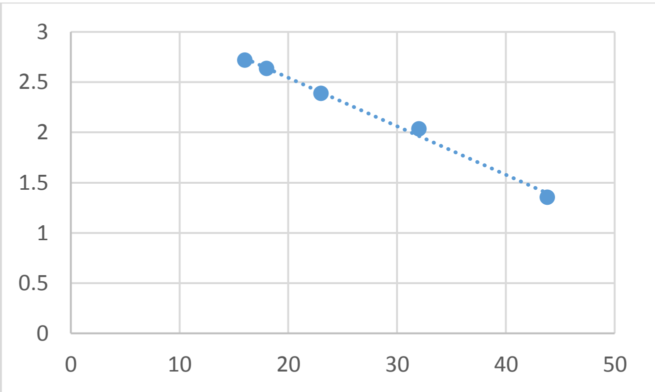

Fig. 18. Lmax VS FOS Graph

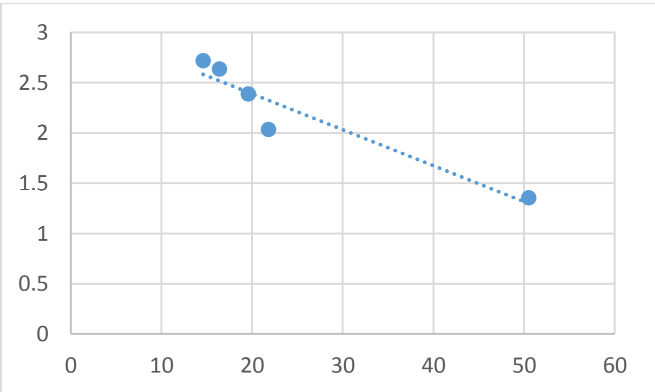

Fig. 19. Excavation Inclination VS FOS Graph

Sensitivity to Model Parameters: The factor of safety can be sensitive to various model parameters, including pore water pressure conditions, groundwater conditions, and strength parameters. Small changes in these parameters can result in different factor of safety values. [2]

3.2. GEOSLOPE:

Slope stability analysis using GeoSlope software provides a comprehensive assessment of the stability of slopes. The software utilizes various methods and algorithms to analyze the geotechnical factors affecting slope stability. By inputting relevant data such as soil properties, groundwater conditions, and slope geometry, the software performs calculations to determine the factor of safety and assess the potential for slope failure.

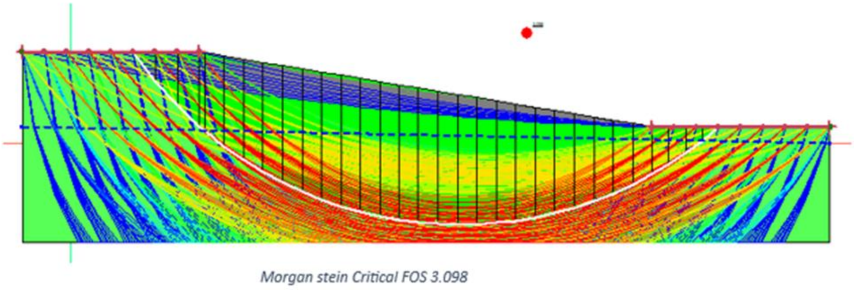

Fig. 20. Morganstein Critical FOS 3.098

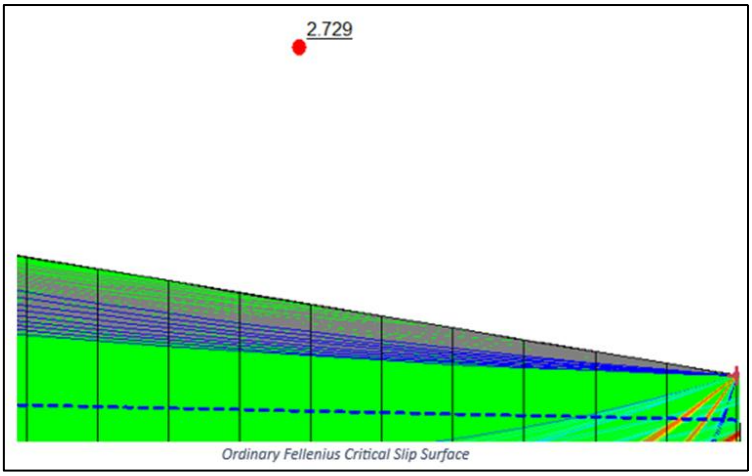

Fig. 21. Ordinary Fellenius Critical Slip Surface FOS 2.729

Table 16. Geoslope FOS (from fig 20-21)

Software Employed	Geoslope	
Method Type	Morgenstern-Price method	Ordinary or Fellenius method
Factor of Safety	3.098	2.792

GeoStudio and PLAXIS 2D may employ different calculation methods for slope stability analysis. GeoStudio's Slope/W module typically uses limit equilibrium methods, such as the Bishop method or the Modified Bishop method. PLAXIS 2D, on the other hand, employs finite element analysis coupled with either limit equilibrium or stress-based methods. The differences in calculation methods can lead to variations in the factor of safety values obtained.

4. Conclusion

Based on the first evaluation as per Chinese criteria, the soil at various depths was found to be not susceptible to liquefaction, whereas the second evaluation as per Modified Chinese criteria gave different and more specific results taking into the % clay-sized particles. Based on Modified Chinese criteria, the soils ranging from 10-20 ft, 25-30 ft and 30-35 ft were found explicitly as non-susceptible, whereas soil ranging from 0-10 ft and 20-25 ft requires further study on non-plastic clay-sized grains as per the criteria.

Considering Figure 12-16 in PLAXIS2D, the increase in factor of safety was observed due to;

1. Increase in body mass of soil at toe of slope
2. Decrease in angle of the slope (Gentle Slope) (Affects FOS of original slope)
3. Decrease in foot/toe length of the slope
4. Decrease in Loading area
5. Increase in Soil strength parameters
6. Decrease in Soil cut slope angle (Gentle Slope) (Affects FOS of cut slope with/without surcharge)
7. FOS of original slope is reduced by decreasing the area of load on top of slope
8. FOS of Excavated surcharge is increased by doing point 7
9. Increase in Load area increases factor of safety for the case without surcharge up to a certain extent,
10. Increasing toe area decreases the FOS for both cases (with/without surcharge)
11. Observing the deformed mesh and total displacement mesh it could be seen where could be the problem in factor of safety and loading surcharge. Upon modification, FOS substantially increased.

Considering characteristic value of shear strength, the factor of safety should be greater than 1.35 as per DA3 approach of EC7 standard. As obtained from both finite element (i.e. PLAXIS2D) and limit equilibrium (i.e. GEOSLOPE), we can conclude the safety of designed slope.

References

[1] I. "James R. Martin, “High-Modulus Columns for Liquefaction Mitigation,” JOURNAL OF GEOTECHNICAL AND GEOENVIRONMENTAL ENGINEERING © ASCE / JUNE 2004, 2004.
[2] B. Chakrabarti, S. Puppanna, and P. Scholar, “TWO-DIMENSIONAL SLOPE STABILITY ANALYSIS WITH VARYING SLOPE ANGLE AND SLOPE HEIGHT BY PLAXIS-2D,” p. 659, May 2017.
[3] B. A. Mohaymin Sahito -, “LIQUEFACTION EVALUATION FOR FOUNDATION DESIGN AND SOIL IMPROVEMENT MEASURES,” 2014.
[4] A. Marto and T. Soon, “Short Review on Liquefaction Susceptibility,” International Journal of Engineering Research and Applications (IJERA), vol. 2, no. 3, pp. 2115–2119, 2012, [Online]. Available: http://www.ijera.com/papers/Vol2_issue3/MM2321152119.pdf
[5] H. B. Seed and I. M. Idriss, “Ground Motions and Soil Liquefaction During Earthquakes,” 1982. [Online]. Available: https://api.semanticscholar.org/CorpusID:127517600
[6] D. C. Andrews and G. R. Martin, “CRITERIA FOR LIQUEFACTION OF SILTY SOILS,” 1999. [Online]. Available: https://api.semanticscholar.org/CorpusID:54170395
[7] B. M. Das, “Principles of geotechnical engineering / Braja M. Das,” 2007. [Online]. Available: https://api.semanticscholar.org/CorpusID:107277683
[8] R. Green and K. Ziotopoulou, “Overview of screening criteria for liquefaction triggering susceptibility,” May 2015.
[9] E. Altalhe, “Lecture (2) | Particle Analysis for Fine soil (Hydrometer Analysis),” May 2023.
[10] F. S. Niazi, A. Pinan-Llamas, and B. Sulaman, “Revisiting the Liquid Limit Determinations Using Casagrande Percussion Cup Method vs. Fall Cone Device,” in Geo-Congress 2022, pp. 152–161. doi: 10.1061/9780784484036.016.
[11] S. Puppanna, A. Ragavendra, Rakeshm, and V. B R, “Slopes Stability Analysis Using the Plaxis 2D Program and Taylor’s Stability Equation,” May 2020.

Authors’ Profiles

Sheeraz Ahmed Rahu has an MSc in Structural Engineering from Budapest University of Technology and Economics. His specialization is in Geotechnics and Engineering Geology. His research areas include Highway Structural Design, Sustainability in Concrete Construction, Life Cycle Assessment of Pavement Construction, Soil Liquefaction Susceptibility.

Zaheer Ahmed Almani works as a Professor at the Department of Civil Engineering, Mehran University of Engineering and Technology, Jamshoro, Pakistan. His research areas include numerical modeling and physical testing in geotechnical engineering. Key areas include shallow foundation behavior in unsaturated and multi-layer soils, soil stabilization techniques using polypropylene fibers and waste materials, and liquefaction susceptibility. Studies also explore foundation settlement, swelling, and improvements for geotechnical properties under varied soil conditions.

Muhammad Rehan Hakro works as a Lecturer at the Department of Civil Engineering, Mehran University of Engineering and Technology, Jamshoro, Pakistan. His research areas include numerical and experimental modeling in geotechnical and civil engineering, with a focus on soil stability, unsaturated soil behavior, and foundation design. His research covers soil stabilization, liquefaction susceptibility, rainfall-induced slope failures, and hydrological effects on foundations, advancing sustainable practices in complex soil conditions.

How to cite this paper: Sheeraz Ahmed Rahu, Zaheer Ahmed Almani, Muhammad Rehan Hakro, "Liquefaction Susceptibility of Earthworks Site: Numerical Modelling of Embankment Cut by PLAXIS2D and GEOSLOPE Using Eurocode 7", International Journal of Engineering and Manufacturing (IJEM), Vol.15, No.2, pp. 1-18, 2025. DOI:10.5815/ijem.2025.02.01